CLINICAL ARTICLE

Application of 3D-printed Customized Guides in Subtalar Joint Arthrodesis

Xiao-jun Duan, MD[1], Hua-quan Fan, BE[1], Fu-you Wang, MD[1], Peng He, ME[2], Liu Yang, MD[1]

[1]Center for Joint Surgery, Southwest Hospital, Third Military Medical University (Army Medical University) and [2]Chongqing Institute of Optics and Mechanics, Chongqing, China

Objective: To explore the feasibility of 3D printed customized guides assisting the precise drilling of Kirschner wires in subtalar joint arthrodesis.

Methods: We retrospectively reviewed the data of 29 patients (30 subtalar joints) who underwent subtalar joint arthrodesis between 1 July 2013 and 31 December 2017. The customized guides were designed on a full-scale 3D polylactic acid model made from computed tomography (CT) data of patients by Model Intestinal Microflora in Computer Simulation (MIMICS) software, which were manufactured by 3D printing technology. A total of 14 joints used customized guides (experimental group); the remained 16 joints used the traditional method (control group). The time of drilling the Kirschner wires to the correct position, the time of subtalar fusion, American Orthopaedic Foot & Ankle Society (AOFAS) scores, and complications were evaluated in both groups.

Results: All customized guides were successfully manufactured. In the experimental group, it took 2.1 ± 0.7 min to drill the Kirschner wire to the satisfactory position, and 2 cases needed to be re-drilled; in the control group, it took 4.6 ± 1.9 min to drill the Kirschner wire to the satisfactory position ($P < 0.05$), and 8 cases needed to be re-drilled. No serious complications occurred in both groups during and after the surgery. Postoperative radiographic fusion was confirmed in all cases. No significant difference was observed in the fusion time and AOFAS scores 1 year postoperatively between the two groups ($P > 0.05$).

Conclusion: It is safe to apply 3D-printed customized guides for subtalar joint arthrodesis, which can assist the accurate drilling of Kirschner wires into the appropriate position according to the preoperative plan, and reduce the operation time as well as intraoperative radiation.

Key words: 3D printing; Customized guide; Subtalar joint; Arthrodesis

Introduction

The subtalar joint is an important weight-bearing joint in the foot and ankle. Local pain of the subtalar joint, limping, and varus or valgus deformity may occur when there is extensive damage of the articular cartilage in the subtalar joint due to trauma, degeneration, or other reasons. Patients with mild symptoms or a shorter duration (<6 months) can be cured conservatively, such as with braces, rest, and topical or oral painkillers. However, surgical treatment is needed when those conservative treatments fail. Because the subtalar joint is the amphiarthrodial joint and there is currently no ideal prosthesis for subtalar joint arthroplasty, subtalar joint arthrodesis is a reliable and effective operative strategy for end-stage subtalar disorder[1–6]. The key point for this procedure is the precise position of the fixation screws[1,7].

Internal fixation with cannulated screws is the most frequently used fixation method for subtalar joint arthrodesis. Accurate drilling of the Kirschner wire is the prerequisite for ensuring the satisfactory position of the screw. After the anatomical reduction of the subtalar joint and with the posterior malleolus kept in the functional position, the surgeon percutaneously drills the Kirschner wire to temporarily fix

Address for correspondence Xiao-jun Duan, MD, Center for Joint Surgery, Southwest Hospital, Third Military Medical University (Army Medical University), No. 30 Gaotanyan Street, Shapingba District, Chongqing, China 400038 Tel: 86-23-68765290; Fax: 86-23-68765293; Email: duanxiaojun@hotmail.com

Disclosure: This study was funded by the Chongqing Science and Technology Commission Fund (No. CSTC, 2016shmszx0630) and the Southwest Hospital Fund (Nos. SWH2016BZGFGJJ-02, SWH2017JSZD-05).
Received 24 July 2018; accepted 31 October 2018

the position for subtalar joint arthrodesis, and then determines whether the position of the Kirschner wire is satisfactory by C-arm fluoroscopy. The Kirschner wire needs to avoid entering the ankle surface or neurovascular injury. The cannulated screw that goes through the Kirschner wire should be supported by bone of sufficient strength to achieve firm fixation. Traditionally, the drilling of the Kirschner wire is dependent on bony anatomical marks and previous experience of surgeons. C-arm fluoroscopy is frequently used during the operation to confirm the position of the wires, which would not only extend the operation time but also increase the intraoperative radiation. The application of customized guides that are highly matched with the patients' anatomical morphology are emerging as a new strategy to achieve the accurate drilling of Kirschner wire and address the above concerns. 3D printing technology is a new rapid prototyping technology, but its medical application is well developed[8–11]. However, few have reported on the use of 3D-printed customized guides to improve the efficacy of subtalar joint arthrodesis.

In this study, we utilize the bony anatomical morphology from the patients' CT scans to manufacture customized guides for subtalar joint arthrodesis. The aim of our preliminary study is: (i) to investigate the efficacy of 3D-printed customized guides; (ii) to clarify the safety of the 3D-printed customized guides; and (iii) to provide reference for the promotion and application of this technology.

Materials and Methods

Inclusion and Exclusion Criteria

The inclusion criteria were: (i) patients were primarily diagnosed as having traumatic, degenerative or rheumatoid subtalar arthritis; (ii) weight-bearing radiograph of the lateral view showed narrow space in the subtalar joint, or Short-TI Inversion Recovery (STIR) MRI suggested osteoarthritis (OA) in the subtalar joint; (iii) the treatment for the patient was subtalar joint arthrodesis; (iv) outcomes are drilling time of the Kirschner wires to the correct position, subtalar fusion time, American Orthopaedic Foot & Ankle Society (AOFAS) scores and complications; and (v) retrospective study.

The exclusion criteria were: (i) obvious degeneration in ankle or talonavicular joint; (ii) complications of ischemic necrosis of the talus; (iii) abnormality of lower extremity muscle strength; (iv) subtalar joint tuberculosis, infection, tumor, or Charcot joint disease; (v) multiple joints that required arthrodesis; (vi) obvious coagulation abnormality; (vii) skin and soft tissue infections; and (viii) the subtalar joint was not painful after 3 months of conservative treatment.

Participants

We retrospectively reviewed the medical data of patients who underwent subtalar joint arthrodesis between 1 July 2013 and 31 December 2017 in our center. A total of 29 patients were enrolled, including 13 men and 16 women. One case had bilateral lesions in the subtalar joint, which was operated on separately; the rest were unilateral lesions. All operations were performed by the same senior surgeon. Patients were divided into two operative groups: a customized guide group (experimental group) and a traditional method group (control group).

All procedures performed in studies involving human participants were in accordance with the ethical standards of the institutional and/or national research committee and with the 1964 Helsinki declaration and its later amendments or comparable ethical standards. The research was registered on www.clinicaltrials.gov (NCT03152916). Informed consent was obtained from all individual participants included in the study.

Preoperative Examination of Images

Routine radiographs of anteroposterior, lateral, and posterior views of the subtalar joint in standing position were taken to assess the alignments and subtalar joint space. MRI of the subtalar joint was routinely performed using Artoscan C (0.2T, Esaote, Italy) to assess cartilage and bone conditions, and whether there was manifestation of OA in the adjacent ankle and talonavicular joint. Usually the STIR MRI revealed high signal intensity of edema in tissues on both sides of the subtalar joint.

Preoperative radiographs suggested narrow joint space and forming of osteophyte. Preoperative MRI suggested subtalar joint degeneration; edema near the articular surface of the calcaneus and talus; and subtalar joint effusion, sometimes accompanied by bone defects.

Preoperative Preparation of Customized Guide

Three-dimensional thin-layer CT scan (Siemens, Germany) of the subtalar joint was routinely performed, and the CT scan slice thickness was 1 mm. The Digital Imaging and Communications in Medicine (DICM) data was extracted and imported into the Model Intestinal Microflora in Computer Simulation (MIMICS) software to reconstruct the 3D data of the subtalar joint and its surrounding bone and soft tissue. The MIMICS-reconstructed data was imported into the 3D design software SIEMENS NX (Siemens PLM Software, Germany) to design the guides for subtalar joint arthrodesis. The guide consisted of two parts. One was the calcaneal guide plate, which was prepared based on the patient's anatomy of calcaneus; it was highly conformed to the surface morphology of calcaneus and had positioning holes for Kirschner wire drilling. The other one was the positioner that could determine the position of the Kirschner wire (Fig. 1).

The data of the designed guides were converted into STL format and imported into a 3D printer (Model: UP BOX, Tiertime, China) for printing. Polylactic acid (Tiertime, China) was used as a raw material. The customized guides for subtalar joint arthrodesis (Fig. 2) were printed, sealed, and sterilized with ethylene oxide for intraoperative use.

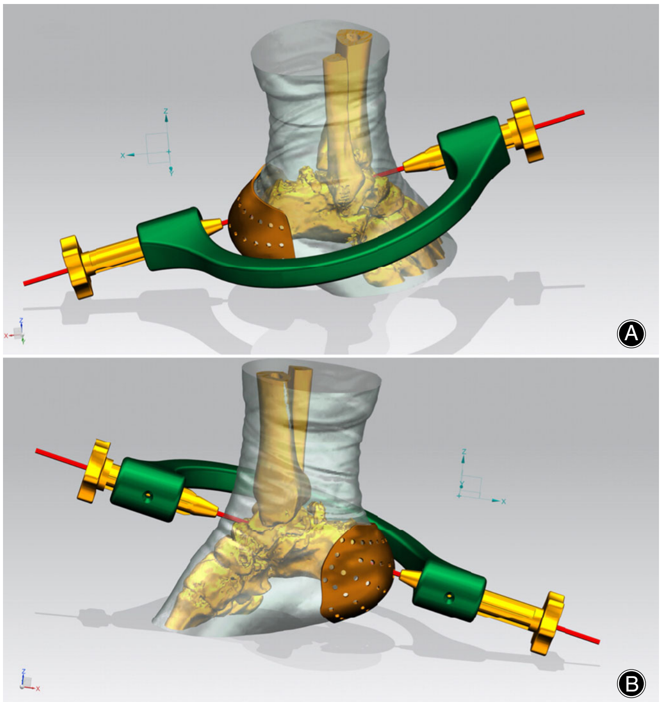

Fig. 1 Design and preparation of the customized guides. Design the customized guide for subtalar arthrodesis with the aid of computer software.

Operative Techniques

Anesthesia and Position

Nerve block anesthesia, epidural anesthesia, or general anesthesia were conducted for all patients. Patients were positioned in the semilateral decubitus position with a thigh tourniquet. The hip on the affected side was moderately elevated, allowing a slightly internal rotation of the lower extremity to the operating table. After routine sterilization and draping, the arteria dorsalis pedis was marked out on the skin with a marker. The tourniquet pressure was 280–300 mmHg. The contralateral lower limb lay flat on the operating table. The position of the patient must facilitate the intraoperative fluoroscopy.

Approach and Exposure

The incision was marked, which was usually a sinus tarsi incision below the lateral malleolus. A curvilinear incision of 5–6 cm was marked toward the base of the fourth metatarsal. The skin, subcutaneous tissue, and articular capsule were incised layer by layer. When incising the articular capsule, care must be taken to not injure the peroneal tendons by pulling it posteriorly and distally with a retractor. After removing the fat in the sinus tarsi area, a lamina spreader was placed into the subtalar joint.

Pathological Changes and Resection

Articular cartilage defects and synovial hyperplasia were observed during the surgery. All cartilage of the posterior facets in the subtalar joint must be scraped using a curette.

Fig. 2 Customized guide apparatus for subtalar arthrodesis prepared by 3D printing.

A 1.5-mm Kirschner wire was used to drill in the fusion facet to facilitate the penetration of bone marrow. After flushing the subtalar joint, an appropriate amount of allograft cancellous bone can be implanted in the posterior facet of the subtalar joint. Then the laminar spreader can be removed and the subtalar joint can be reset to the functional position.

Fixation

According to Coughlin *et al.*, we used two cannulated screws to fix the subtalar joint in this series[12]. The position of the screws was guided by two 2.0-mm Kirschner wires that were already in satisfactory position. The first Kirschner wire often passed through the superior calcaneal tuberosity, the posterior articular surface of the subtalar joint, then the talar neck. The second Kirschner wire often passed through the medial side of the talar neck and calcaneus. With the help of the 3D-printed positioner, the precise position of the Kirschner wires could be easily determined and marked. Attention should be paid to avoid the arteria dorsalis pedis. The control group drilled in the Kirschner wires without any guides, just relying on the positioning mark on the skin surface as well as the experience of the surgeon. C-arm fluoroscopy was applied to confirm that the subtalar joint was ideally reset and the Kirschner wires were passed through satisfactorily. Then the incision was moderately enlarged for screw insertion, and two cannulated screws of 7.5 mm in diameter (General Care, China) were inserted through the Kirschner wires. Before the end of the operation, C-arm fluoroscopy was used to confirm the length of the screws. The articular capsule and subcutaneous tissue were closed layer by layer. All incisions were interruptedly sutured with nylon sutures. Plaster cast below the knee joint was used for immobilization.

Postoperative Treatment

The patients received intravenous antibiotics for 24 h according to the instructions. The operated limb was elevated after the operation. Early exercise without weight-bearing was acceptable, such as quadriceps contraction and leg lifting, to prevent muscle atrophy and lower extremity thrombosis. The stitches were taken out 2 weeks postoperatively; the plaster immobilization was continued and was taken off 6 weeks postoperatively when radiographs showed bony callus growth; weight-bearing walking could be conducted with the protection of walking boots (Aircast, USA) for 4–6 weeks. Patients were evaluated clinically and radiographically until union was achieved or the diagnosis of nonunion was established by CT. Clinically, fusion was defined by subtalar joint stability without any symptoms. Radiographically, fusion was defined as obliteration of the subtalar joint space with the presence of crossing trabeculae. CT criteria for fusion was consolidation of at least 50% of the posterior facet of the subtalar joint. All suspected cases of delayed union or nonunion were evaluated by CT. If union was confirmed *via* radiographs, the patients could walk with full weight-bearing. The AOFAS scores of the patients were obtained preoperatively and at 1 year postoperatively.

Outcome Measures

Kirschner Wire Drilling

Drilling time of the Kirschner wires to the correct position was recorded during the surgery to investigate efficacy of the guides in shortening surgery time and reducing intraoperative fluoroscopy times.

Subtalar Fusion Time

Radiographic examinations were conducted in the regular follow-ups to record the union time of the patients.

American Orthopaedic Foot & Ankle Society scores and Complications

The AOFAS scores before and after surgery and the occurrence complications postoperatively were also recorded to evaluate the efficacy and safety of the guides.

Statistical Methods

The continuous variances are presented as mean ± SD and statistical analysis was performed using SPSS 13.0 (SPSS, Chicago, IL, US). A two-sided Student's *t*-test was used to compare the drilling time of Kirschner wires, the union time, and AOFAS scores between the two groups. Significance was determined as $P < 0.05$.

Results

General Results

The 3D-printed customized guides based on patients' subtalar joint CT data were successfully manufactured. There were no significant differences in age, course of disease, and preoperative AOFAS scores between the two groups. All 29 patients were followed for 1.8 ± 0.7 years (range, 1–3 years).

Drilling Time of the Kirschner Wires

In the experimental group, only 2 cases required re-drilling of the Kirschner wire and it took 2.1 ± 0.7 min to drill the Kirschner wire to the satisfactory position; the reason the Kirschner wire in these 2 cases needed to be re-drilled was mainly due to the insufficient strength of the guide that led to deviation. In the control group, 8 cases required re-drilling of the Kirschner wire and the mean time was 4.6 ± 1.9 min ($P < 0.05$).

TABLE 1 The two groups' comparative follow-up study

Groups	Subtalar joint arthrodesis (n)	Age (y)	Course of disease (y)	Time of drilling the Kirschner wire (min)	Intraoperative fluoroscopy times	Time of bony fusion (wk)	Preoperative AOFAS Scores (pt)	Postoperative 1 year AOFAS Scores (pt)
Experimental group	14	52 ± 19	4.2 ± 2.1	2.1 ± 0.7	2.4 ± 0.2	14 ± 3	60 ± 5	89 ± 5
Control group	16	50 ± 18	3.9 ± 2.2	4.6 ± 1.9	3.5 ± 0.8	13 ± 2	59 ± 8	88 ± 6
P-value		$P > 0.05$	$P > 0.05$	$P < 0.01$	$P < 0.01$	$P > 0.05$	$P > 0.05$	$P > 0.05$

AOFAS, American Orthopaedic Foot & Ankle Society.

Subtalar Fusion Time and American Orthopaedic Foot & Ankle Society Scores

Postoperative radiograph confirmed union in all cases. The union time of the two groups was 13–14 weeks. No significant difference was observed in subtalar fusion time and AOFAS scores at 1 year postoperatively between the two groups ($P > 0.05$). The AOFAS scores of the two groups had significant differences compared with those before surgery.

Complications

There was no neurovascular injury or other complications (such as poor wound healing, infection, or deep vein thrombosis of the lower extremities) in both groups. The comparative study of the two groups is shown in Table 1.

Typical Cases

Case 1

A 51-year-old man was admitted to the hospital because of "traumatic right subtalar pain associated with limitation of motion for 2 years." Conservative treatment in another hospital failed. Preoperative diagnosis was right calcaneal fracture malunion with secondary traumatic subtalar arthritis. We manufactured the 3D-printed customized guide for him and conducted subtalar joint arthrodesis with the help of the

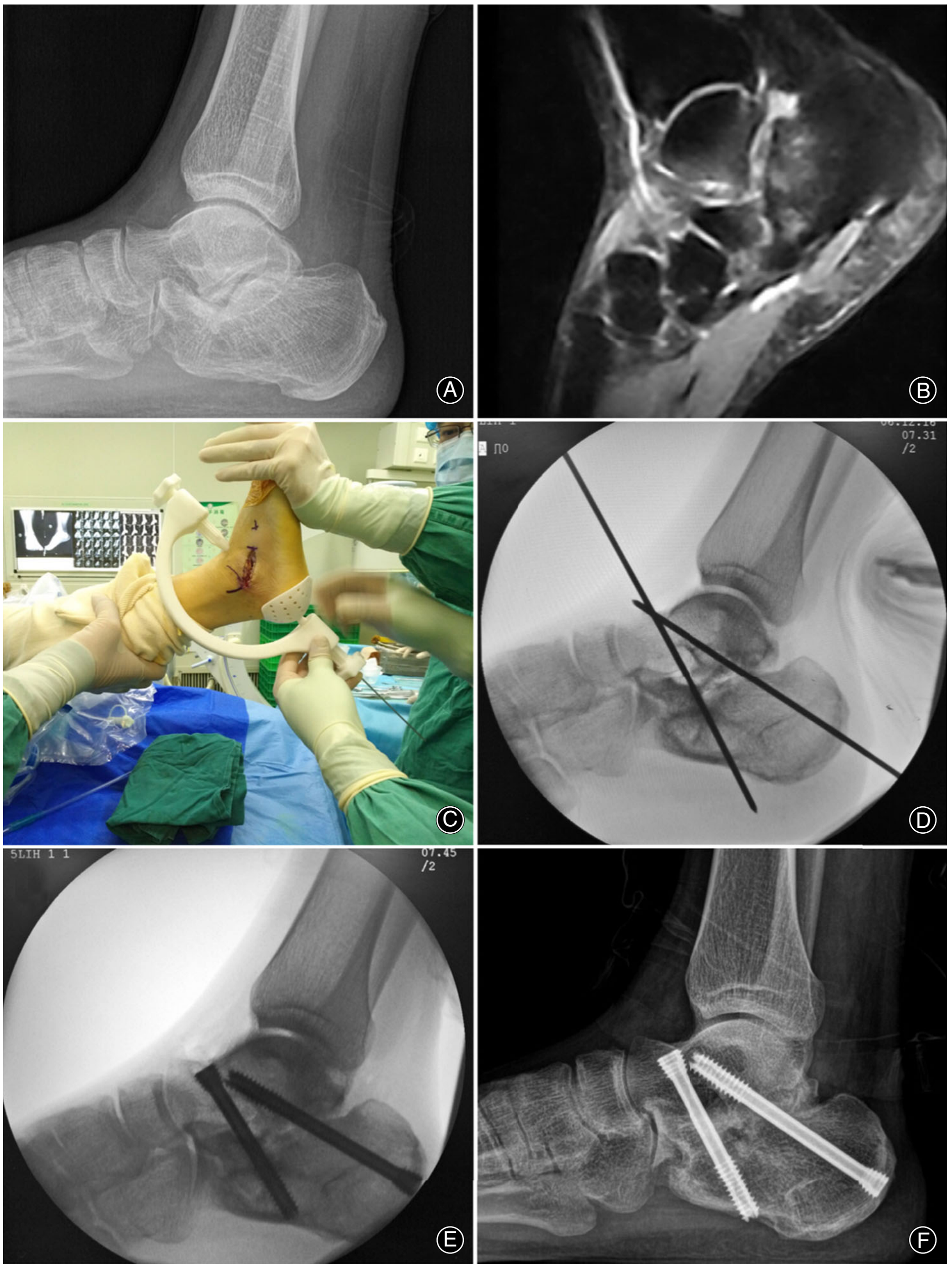

Fig. 3 Typical case 1: (A) Preoperative lateral view radiograph of the subtalar joint showing narrow space of the joint; (B) preoperative Short-TI Inversion Recovery (STIR) MRI suggesting osteoarthritis in subtalar joint; (C) using customized guides to determine the position of Kirschner wires; (D) intraoperative C-arm fluoroscopy confirming that the position of the Kirschner wires were satisfactory and the subtalar reduction was ideal; (E) the position and length of the cannulated screws were confirmed by C-arm fluoroscopy before closing the incision; and (F) radiograph at 1 year postoperatively suggesting subtalar bony fusion and the obliteration of subtalar joint space.

guide (Fig. 3). The patient's AOFAS score increased from 65 points preoperatively to 95 points 1 year postoperatively.

Case 2

A 74-year old woman was admitted to the hospital because of "right ankle pain due to ankle sprain and limitation of motion for 1 year". She was diagnosed as having "right subtalar joint traumatic arthritis, osteoporosis". We manufactured the 3D-printed customized guide according to her ankle joint CT data and conducted right subtalar joint arthrodesis with the help of the guide. The Kirschner wire was drilled with the aid of the guide; the cannulated screws were inserted after the position of the wires and were confirmed by C-arm fluoroscopy. Radiographic re-examination at 3 months postoperatively showed that the subtalar bony fusion was achieved (Fig. 4).

Case 3

A 46-year-old woman was admitted to the hospital because of "left ankle pain for more than 27 years, exacerbated for more than 2 years". She was diagnosed with "left subtalar joint severe OA". A 3D image was obtained from ankle joint CT data, and a customized guide was designed. The patient underwent arthroscopic left subtalar arthrodesis. The Kirschner wire was drilled with the aid of the 3D-printed guide, and the cannulated screw was inserted. Radiographic

Fig. 4 Typical case 2: (A,B) Preoperative radiographs of the patient when admitted to hospital; (C) using customized guides to help drill the Kirschner wires; (D) intraoperative C-arm fluoroscopy confirming that the position of the Kirschner wires was satisfactory; and (E,F) radiographs at 3 months postoperatively suggesting the completion of subtalar bony fusion.

re-examination at 3 months postoperatively showed that subtalar bony fusion was achieved (Fig. 5).

Discussion

Subtalar arthrodesis has been considered the most successful method for treating calcaneal malunion, traumatic subtalar arthritis, primary OA, rheumatoid arthritis, and hindfoot deformity, with low incidence of complications[1,13–16]. The operative techniques of subtalar arthrodesis are as follows: (i) Selection of incision: When performing *in situ* arthrodesis, selecting the sinus tarsi incision[16–19]; when performing distraction arthrodesis, selecting the lateral malleolus incision. (ii) Exposure of joint space: The lamina spreader is inserted into the joint space and then gradually enlarged to allow better visualization of the joint space[1,16,20,21]; if it is difficult to enter the subtalar joint space, positioning with the help of C-arm fluoroscopy is necessary. (iii) Fixation method: Cannulated screw is still the dominant method for fixation[1,5,16]. Jastifer *et al.* showed that two unparalleled screws could achieve the strongest mechanical stability, and the strength of three screws was greater than two[7,22,23]. For patients with uncollapsed subtalar articular surfaces, it does not seem particularly important for bone grafting[24], but for cases with subtalar joint collapse, the distraction of posterior subtalar joint and bone grafting is important[1,25].

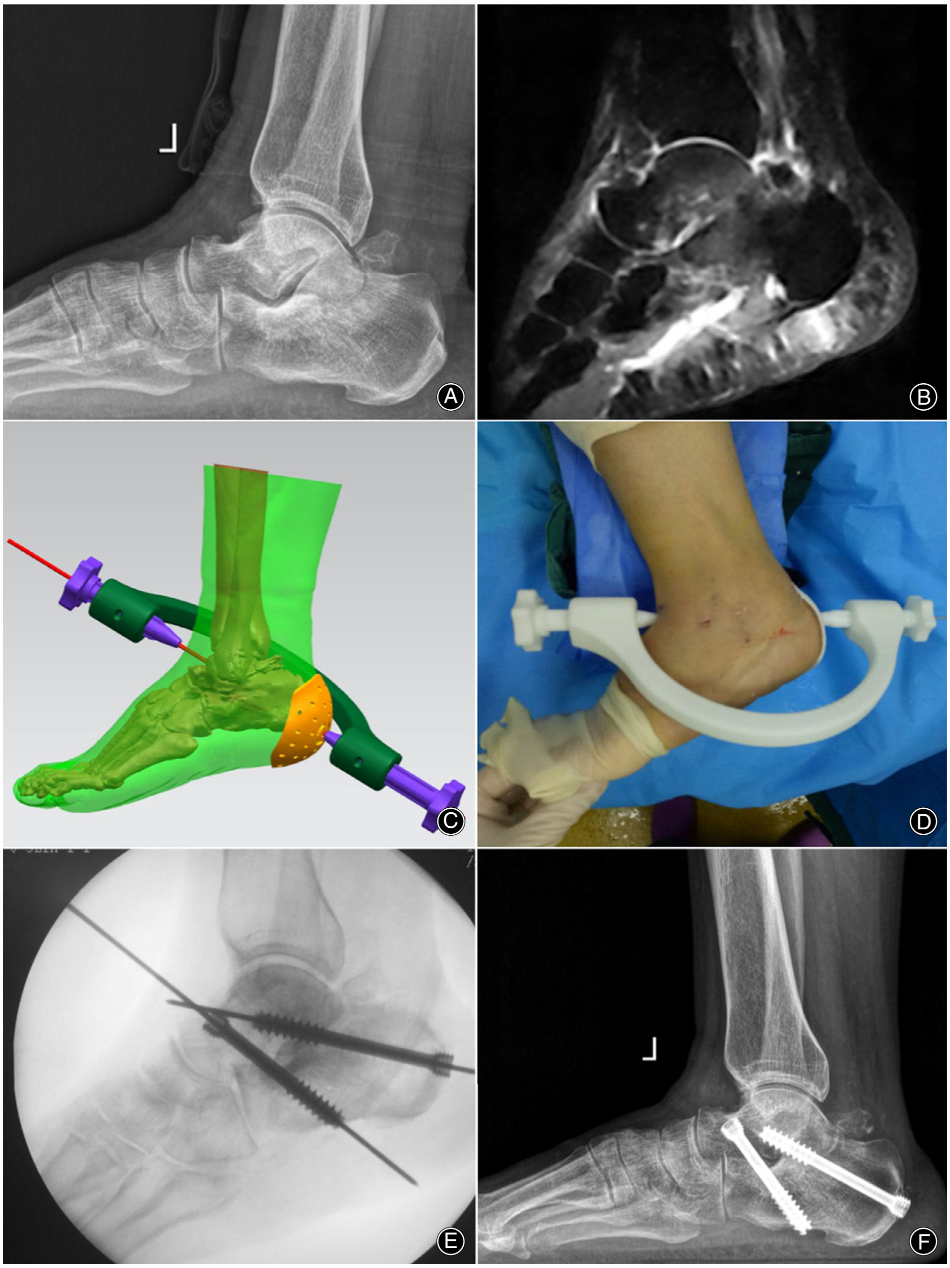

Fig. 5 Typical case 3: (A) Preoperative lateral view radiograph of the subtalar joint; (B) preoperative MRI of the subtalar joint; (C) customized guides designed in the computer software; (D) using customized guides to help drill the Kirschner wires; (E) cannulated screw screwed in for fixation; and (F) radiographs at 3 months postoperatively suggesting the completion of subtalar bony fusion.

To insert the cannulated screw in satisfactory position, the Kirschner wire needs to be drilled in the ideal position[4]. Previously, surgeons have usually drilled the wire according to their experience, and frequently used the C-arm fluoroscopy to confirm whether the position of the wires was satisfactory; if not, drilling would be redone. This leads to prolonged operative time and increased intraoperative radiation, which is harmful for both surgeons and patients. 3D printing technology has brought new hope for achieving precise drilling of Kirschner wires. The application of 3D printing technology in orthopaedic surgery is developing rapidly and has been successfully used in many medical fields, such as for clearer 3D demonstration of disease and operation plans for doctor–patient communication[26–29]; for preparation of a large amount of customized casts and insoles[30]; manufacture of guides that are highly matched with the anatomy of the patient, which facilitates the positioning of implants and reduces the operation time[31]; and printing of customized metal implants to improve operative outcomes[32,33]. To prepare the customized guides, we need to first collect the CT data of the patient to conduct the 3D image reconstruction. The engineer must fully understand the purpose of the operation so that the guides can be successfully manufactured according to the surgeon's plan, thus conducting a simplified and effective operation[34–42]. The manufactured guide should be sterilized before surgery. This study suggests that 3D-printed customized guides designed and manufactured based on patients' CT data can simplify the key operative procedures without compromising the outcome[41]. This is a recommended technique, especially for inexperienced surgeons. The use of customized guides could reduce the trauma of the operation, shorten the operation time, and reduce the frequency of using C-arm fluoroscopy during surgery, thus reducing the adverse effects of intraoperative radiation. There were still two cases in the experimental group where the position of the Kirschner wires was re-adjusted and re-drilled. The reason may be that the rigidity of the guides made by polylactic acid was insufficient. If they were made of hard metal, the probability of error would be reduced.

There are still some limitations in this study. Because CT scans need to be conducted to prepare the 3D-printed guides, the medical costs will increase. In addition, this study is a retrospective case study, not a prospective randomized controlled study; the number of cases and participating research units in the study are limited. Future multi-center prospective randomized controlled studies need to be conducted to overcome these deficiencies.

Acknowledgments

The authors thank Xin Chen from the Center for Joint Surgery, Southwest Hospital, Third Military Medical University (Army Medical University) for the language support and help.

References

1. Catanzariti AR, Mendicino RW, Saltrick KR, Orsini RC, Dombek MF, Lamm BM. Subtalar joint arthrodesis. J Am Podiatr Med Assoc, 2005, 95: 34–41.
2. Grice DS. Further experience with extra-articular arthrodesis of the subtalar joint. J Bone Joint Surg Am, 1955, 37-A: 246–259.
3. Thomas FB. Arthrodesis of the subtalar joint. J Bone Joint Surg Br, 1967, 49: 93–97.
4. Buratti RA, Johnson JD, Buratti D. Concurrent ankle and subtalar joint arthrodesis. J Foot Ankle Surg, 1994, 33: 278–282.
5. Duan X, Yang L, Yin L. Arthroscopic arthrodesis for ankle arthritis without bone graft. J Orthop Surg Res, 2016, 11: 154.
6. DiDomenico LA, Butto DN. Subtalar joint arthrodesis for elective and posttraumatic foot and ankle deformities. Clin Podiatr Med Surg, 2017, 34: 327–338.
7. Matsumoto T, Glisson RR, Reidl M, Easley ME. Compressive force with 2-screw and 3-screw subtalar joint arthrodesis with headless compression screws. Foot Ankle Int, 2016, 37: 1357–1363.
8. Peltola SM, Melchels FP, Grijpma DW, Kellomäki M. A review of rapid prototyping techniques for tissue engineering purposes. Ann Med, 2008, 40: 268–280.
9. MacDonald E, Wicker R. Multiprocess 3D printing for increasing component functionality. Science, 2016, 353(6307): aaf2093 -aaf2093. https://doi.org/10.1126/science.aaf2093.
10. Jammalamadaka U, Tappa K. Recent advances in biomaterials for 3D printing and tissue engineering. J Funct Biomater, 2018, 9(1), pii: E22. https://doi.org/10.3390/jfb9010022.
11. Ji Q, Zhang JM, Liu Y, *et al*. A modular microfluidic device via multimaterial 3D printing for emulsion generation. Sci Rep, 2018, 8: 4791.
12. Coughlin MJ, Mann MA, Saltzman CJ, eds. Surgery of the Foot and Ankle, 8th edn. Philadelphia, PA: Mosby, 2007; 1091–1097.
13. Roussignol X. Arthroscopic tibiotalar and subtalar joint arthrodesis. Orthop Traumatol Surg Res, 2016, 102: S195–S203.
14. Romeo G, Martinelli N, Bonifacini C, Bianchi A, Sartorelli E, Malerba F. Recreational sports activities after calcaneal fractures and subsequent subtalar joint arthrodesis. J Foot Ankle Surg, 2015, 54: 1057–1061.
15. Roster B, Kreulen C, Giza E. Subtalar joint arthrodesis: open and arthroscopic indications and surgical techniques. Foot Ankle Clin, 2015, 20: 319–334.
16. Vulcano E, Ellington JK, Myerson MS. The spectrum of indications for subtalar joint arthrodesis. Foot Ankle Clin, 2015, 20: 293–310.
17. Holm JL, Laxson SE, Schuberth JM. Primary subtalar joint arthrodesis for comminuted fractures of the calcaneus. J Foot Ankle Surg, 2015, 54: 61–65.
18. Hentges MJ, Gesheff MG, Lamm BM. Realignment subtalar joint arthrodesis. J Foot Ankle Surg, 2016, 55: 16–21.
19. Lopez R, Singh T, Banga S, Hasan N. Subtalar joint arthrodesis. Clin Podiatr Med Surg, 2012, 29: 67–75.
20. Laporta G, Bock F, Ghate N. Posterior approach for subtalar joint distraction arthrodesis by compact external fixation: a technique guide. J Foot Ankle Surg, 2013, 52: 547–552.
21. Shibuya N, Agarwal MR. Distraction arthrodesis of subtalar joint using a laterally placed hinged distractor. J Foot Ankle Surg, 2012, 51: 820–824.
22. Jastifer JR, Alrafeek S, Howard P, Gustafson PA, Coughlin MJ. Biomechanical evaluation of strength and stiffness of subtalar joint arthrodesis screw constructs. Foot Ankle Int, 2016, 37: 419–426.
23. McGlamry MC, Robitaille MF. Analysis of screw pullout strength: a function of screw orientation in subtalar joint arthrodesis. J Foot Ankle Surg, 2004, 43: 277–284.
24. Shah A, Naranje S, Araoye I, Elattar O, Godoy-Santos AL, Netto CC. Role of bone grafts and bone graft substitutes in isolated subtalar joint arthrodesis. Acta Ortop Bras, 2017, 25: 183–187.
25. Lee MS, Tallerico V. Distraction arthrodesis of the subtalar joint using allogeneic bone graft: a review of 15 cases. J Foot Ankle Surg, 2010, 49: 369–374.
26. Liu ZJ, Jia J, Zhang YG, Tian W, Jin X, Hu YC. Internal fixation of complicated acetabular fractures directed by preoperative surgery with 3D printing models. Orthop Surg, 2017, 9: 257–260.
27. Zang CW, Zhang JL, Meng ZZ, *et al*. 3D printing technology in planning thumb reconstructions with second toe transplant. Orthop Surg, 2017, 9: 215–220.
28. Trauner KB. The emerging role of 3D printing in arthroplasty and orthopedics. J Arthroplasty, 2018, 33: 2352–2354.
29. Ren X, Yang L, Duan XJ. Three-dimensional printing in the surgical treatment of osteoid osteoma of the calcaneus: a case report. J Int Med Res, 2017, 45: 372–380.

30. Cha YH, Lee KH, Ryu HJ, *et al*. Ankle-foot orthosis made by 3D printing technique and automated design software. Appl Bionics Biomech, 2017, 2017: 9610468.
31. Caiti G, Dobbe JGG, Strijkers GJ, Strackee SD, Streekstra GJ. Positioning error of custom 3D-printed surgical guides for the radius: influence of fitting location and guide design. Int J Comput Assist Radiol Surg, 2018, 13: 507–518.
32. Liang H, Ji T, Zhang Y, Wang Y, Guo W. Reconstruction with 3D-printed pelvic endoprostheses after resection of a pelvic tumour. Bone Joint J, 2017, 99-B: 267–275.
33. Ma L, Zhou Y, Zhu Y, *et al*. 3D printed personalized titanium plates improve clinical outcome in microwave ablation of bone tumors around the knee. Sci Rep, 2017, 7: 7626.
34. Naftulin JS, Kimchi EY, Cash SS. Streamlined, inexpensive 3D printing of the brain and skull. PLoS One, 2015, 10: e0136198.
35. Hamid KS, Parekh SG, Adams SB. Salvage of severe foot and ankle trauma with a 3D printed scaffold. Foot Ankle Int, 2016, 37: 433–439.
36. Jastifer JR, Gustafson PA. Three-dimensional printing and surgical simulation for preoperative planning of deformity correction in foot and ankle surgery. J Foot Ankle Surg, 2017, 56: 191–195.
37. Zheng W, Tao Z, Lou Y, *et al*. Comparison of the conventional surgery and the surgery assisted by 3d printing technology in the treatment of calcaneal fractures. J Invest Surg, 2017, 19: 1–11.
38. Martelli N, Serrano C, van den Brink H, *et al*. Advantages and disadvantages of 3-dimensional printing in surgery: a systematic review. Surgery, 2016, 159: 1485–1500.
39. Chung KJ, Huang B, Choi CH, Park YW, Kim HN. Utility of 3D printing for complex distal tibial fractures and malleolar avulsion fractures: technical tip. Foot Ankle Int, 2015, 36: 1504–1510.
40. Li L, Yu F, Shi J, *et al*. In situ repair of bone and cartilage defects using 3D scanning and 3D printing. Sci Rep, 2017, 7: 9416.
41. Duan X, He P, Fan H, Zhang C, Wang F, Yang L. Application of 3D printed personalized guide in arthroscopic ankle arthrodesis. Biomed Res Int, 2018, 2018: 3531293.
42. Zheng W, Chen C, Zhang C, Tao Z, Cai L. The feasibility of 3D printing technology on the treatment of pilon fracture and its effect on doctor-patient communication. Biomed Res Int, 2018, 2018: 8054698.